ELSEVIER

Ultrasonics 40 (2002) 441–448

Ultrasonics

www.elsevier.com/locate/ultras

Piezoelectrically actuated flextensional micromachined ultrasound transducers

Gökhan Perçin [a,*], Butrus T. Khuri-Yakub [b]

[a] *ADEPTIENT, 316 Quinnhill Avenue, Los Altos, CA 94024, USA*
[b] *Edward L. Ginzton Laboratory, Stanford University, Stanford, CA 94305, USA*

Abstract

This paper presents novel micromachined two-dimensional array piezoelectrically actuated flextensional transducers that can be used to generate sound in air or water. Micromachining techniques to fabricate these devices are also presented. Individual unimorph array elements consist of a thin piezoelectric annular disk and a thin, fully clamped, circular plate. We manufacture the transducer in two-dimensional arrays using planar silicon micromachining and demonstrate ultrasound transmission in air at 2.85 MHz with 0.15 μm/V peak displacement. The devices have a range of operating resonance frequencies starting from 450 kHz up to 4.5 MHz. Such an array could be combined with on-board driving and addressing circuitry for different applications.

Keywords: Ultrasound transducers; Micromachining; Piezoelectric actuation; Flextensional transducers; Plate theory; Equivalent circuit; pMUT; PAFMUT

1. Introduction

A schematic of the developed micromachined ultrasound transducer array is shown in Figs. 1 and 2. The individual cell design is based on a flextensional ultrasound transducer that excites the axisymmetric resonant modes of a clamped circular plate. It is constructed by depositing a thin piezoelectric annular plate onto a thin, edge clamped, circular plate. An ac voltage is applied across the piezoelectric material to set the compound membrane into vibration. At the resonant frequencies of the compound membrane, the displacement at the center is large.The transducer array element is made of several cells.

The device is manufactured by silicon surface micromachining and implemented in the form of two-dimensional array. We have designed the fabrication process for piezoelectrically actuated flextensional micromachined ultrasound transducers (PAFMUTs) in a two-dimensional array by combining conventional IC manufacturing process technology with zinc oxide (ZnO) deposition. Individual cells are made of thin silicon nitride membranes covered by a coating of piezoelectric zinc oxide in the form of annular plate that has optimized dimensions. The transducer array element is made of several cells attached in parallel. Materials are chosen in accordance with availability of micromachining and IC manufacturing processes. Other piezoelectric materials, carrier plate materials, electrode metals, and substrates can be used.

2. Design

We have designed the individual cell to have a maximum volumetric displacement of the plate at the resonant frequency. We designed micromachined two-dimensional array transducers learning from the model of a one-element large scale prototype [1–6]. General information about designing unimorph and bimorph transducers, and review of theoretical models can be found in Germano [7] and Denkmann et al. [8]. Analyses of similar devices such as those of Allaverdiev et al. [9], Vassergiser et al. [10], Okada et al. [11] and Iula et al. [12] are helpful in identifying the important parameters of the device. However, the complexity of the structure and the fact that the piezoelectric we use is a ring rather

* Corresponding author. Tel.: +1-650-947-9487.
E-mail address: percin@adeptient.com (G. Perçin).

0041-624X/02/$ - see front matter
PII: S0041-624X(02)00157-9

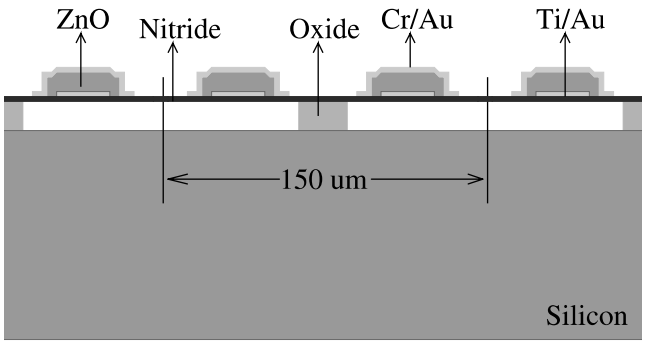

Fig. 1. Side view of two adjacent cells of the developed micromachined two-dimensional array of transducers.

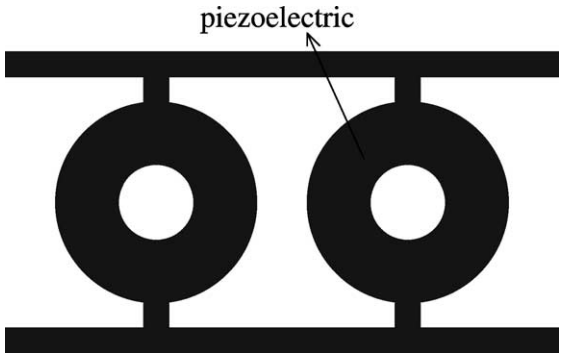

Fig. 2. Top view of the two adjacent cells in Fig. 1.

than a full disk necessitate the use of finite element analysis or complex analytical models to determine the resonant frequencies of the structure, the input impedance of the transducer, and the normal displacement of the surface. Indeed, the complete analysis of the transducer is presented by Perçin and Khuri-Yakub [13].

In the absence of analytical expressions for the equivalent circuit parameters of a flextensional transducer it is difficult to calculate its optimal parameters and dimensions, and to choose suitable materials. The influence of coupling between flexural and extensional deformation, and coupling between the structure and the acoustic volume on the dynamic response of piezoelectrically actuated flextensional transducer are rigorously analyzed using two analytical methods: classical thin (Kirchhoff) plate theory and Mindlin plate theory by Perçin and Khuri-Yakub [13–15]. Classical thin plate theory and Mindlin plate theory are applied to derive rigorous two-dimensional plate equations for the transducer, and to calculate the coupled electromechanical field variables such as mechanical displacement and electrical input impedance. In these methods, the variations across the thickness direction vanish by using the bending moments per unit length or stress resultants. Thus, two-dimensional plate equations for a stepwise laminated circular plate are obtained as well as two different solutions to the corresponding systems. An equivalent circuit of the transducer is also obtained from these solutions. This approach has certain advantages compared to finite element modeling analysis. For instance, a non-linear optimization routine can be developed based on the aforementioned methods.

For an individual cell, by using the parameters of Table 1, we obtain the first resonance frequency at 0.32 MHz, the second at 1.55 MHz, and the third at 4.17 MHz. By using the analysis developed, flexural mode and longitudinal mode transducers are compared in Table 2. The developed flexural mode transducers have larger capacitance, displacement per volt, pressure per volt, volt per pressure, and velocity per volt (zero pressure) compared to conventional longitudinal mode transducers. The results of electrical input impedance and average displacement simulations are given in Figs. 3 and 4 for air, one side water loaded and two sides water

Table 1
Physical dimensions of a typical cell

Dimension	Value (μm)
Radius of the silicon nitride carrier plate	57.5
Inner radius of piezoelectric zinc oxide	15
Outer radius of piezoelectric zinc oxide	40
Thickness of piezoelectric zinc oxide	0.3
Thickness of silicon nitride carrier plate	0.3
Thickness of gold electrodes	0.1

Table 2
Flexural vs. longitudinal mode transducers

	Longitudinal mode transducer cell	Flexural mode transducer cell
Piezoelectric material	PZT 5H Vernitron	Zinc oxide
Relative permittivity	1470	11.1
Transducer area (circular)	0.0104 mm^2	0.0104 mm^2
Piezoelectric thickness	6.35, 1.31, 0.488 mm	0.4 μm
Capacitance (zero strain)	0.02, 0.10, 0.28 pF	2.56 pF
Frequency	0.32, 1.55, 4.17 MHz	0.32, 1.55, 4.17 MHz
Displacement/volt (in air)	81, 17, 6.5 nm/V	370, 160, 320 nm/V
Pressure/volt (in air)	68, 70, 70 Pa/V	303, 645, 3478 Pa/V
Volt/pressure (in air 50 Ω)	87, 88, 87 nV/Pa	380, 810, 4300 nV/Pa
Velocity/volt when $P = 0$ (in air)	0.17, 0.17, 0.17 m/s V	1.3, 8.3, 16.4 m/s V

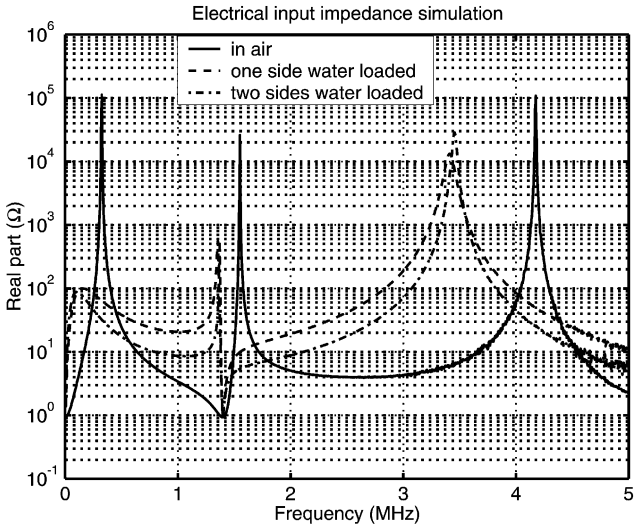

Fig. 3. Electrical input impedance simulation of the single flexural mode transducer cell.

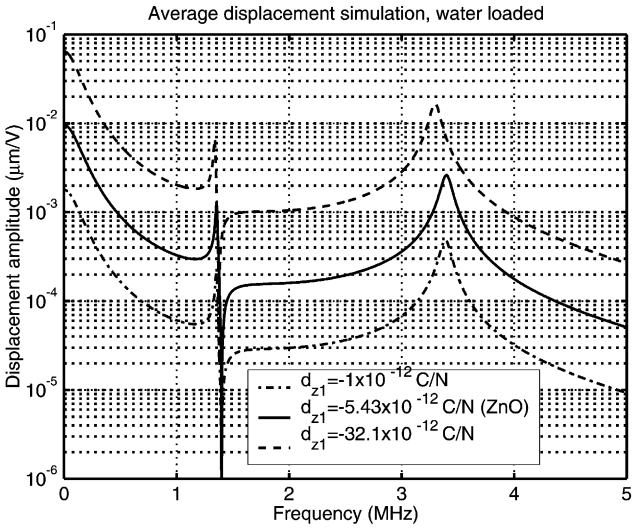

Fig. 5. Average displacement simulation of the single flexural mode transducer cell with different piezoelectric materials with one side water loaded.

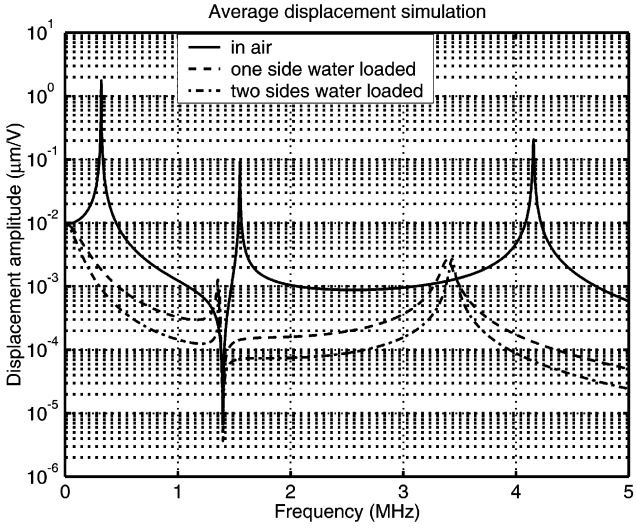

Fig. 4. Average displacement simulation of the single flexural mode transducer cell.

loaded cases. By using different piezoelectric thin film material, average displacement for the one side water loaded case can be increased as shown in Fig. 5, where the average displacement at the second resonance is increased approximately 10 times by using a piezoelectric material with $d_{z1} = -32.1 \times 10^{-12}$ C/N.

3. Fabrication

The fabrication processes for micromachined two-dimensional flextensional transducer arrays are given in Figs. 6 and 7. The first process starts with growing a sacrificial layer, chosen to be silicon oxide (LTO). A non-piezoelectric carrier plate layer of LPCVD silicon nitride is grown on top of the sacrificial layer. Holes for sacrificial layer etching are patterned in the silicon nitride carrier plate layer at the front surface of the wafer by plasma etching. The bottom Ti/Au electrode layer is deposited on the non-piezoelectric carrier plate by e-beam evaporation at relatively high temperature. The degree to which the ZnO c-axis, $\langle 0\,0\,0\,2\rangle$, is oriented normal to the substrate surface is very sensitive to the degree to which the Au film is $\langle 1\,1\,1\rangle$ oriented. Later, the bottom electrode layer is patterned by wet etch, and a piezoelectric ZnO layer is deposited on top of the bottom electrode. The ZnO is deposited by dc planar magnetron sputtering from a zinc target. The deposition is made in an argon-oxygen ambient with a substrate at relatively high temperature. The top Cr/Au electrode layer is formed by e-beam evaporation at room temperature and patterned by liftoff. The last step is etching the sacrificial layer by wet etch, and this concludes the front surface micromachining of the developed devices.

The second fabrication process for micromachined two-dimensional flextensional transducer arrays is given in Fig. 7. The process starts with growing a sacrificial layer, chosen to be silicon oxide (LTO). A non-piezoelectric carrier plate layer of LPCVD silicon nitride is grown on top of the sacrificial layer. Holes for sacrificial layer etching are patterned in the silicon nitride carrier plate layer at the front surface of the wafer by plasma etching. Later, backside access holes are patterned in the silicon nitride and LTO layers at the back surface of the wafer, and the backside access holes are etched by DRIE until reaching the sacrificial silicon oxide layer at the front surface. Because of the material compatibility with the DRIE equipment in our laboratory, we have to choose to etch the backside access holes in bulk silicon

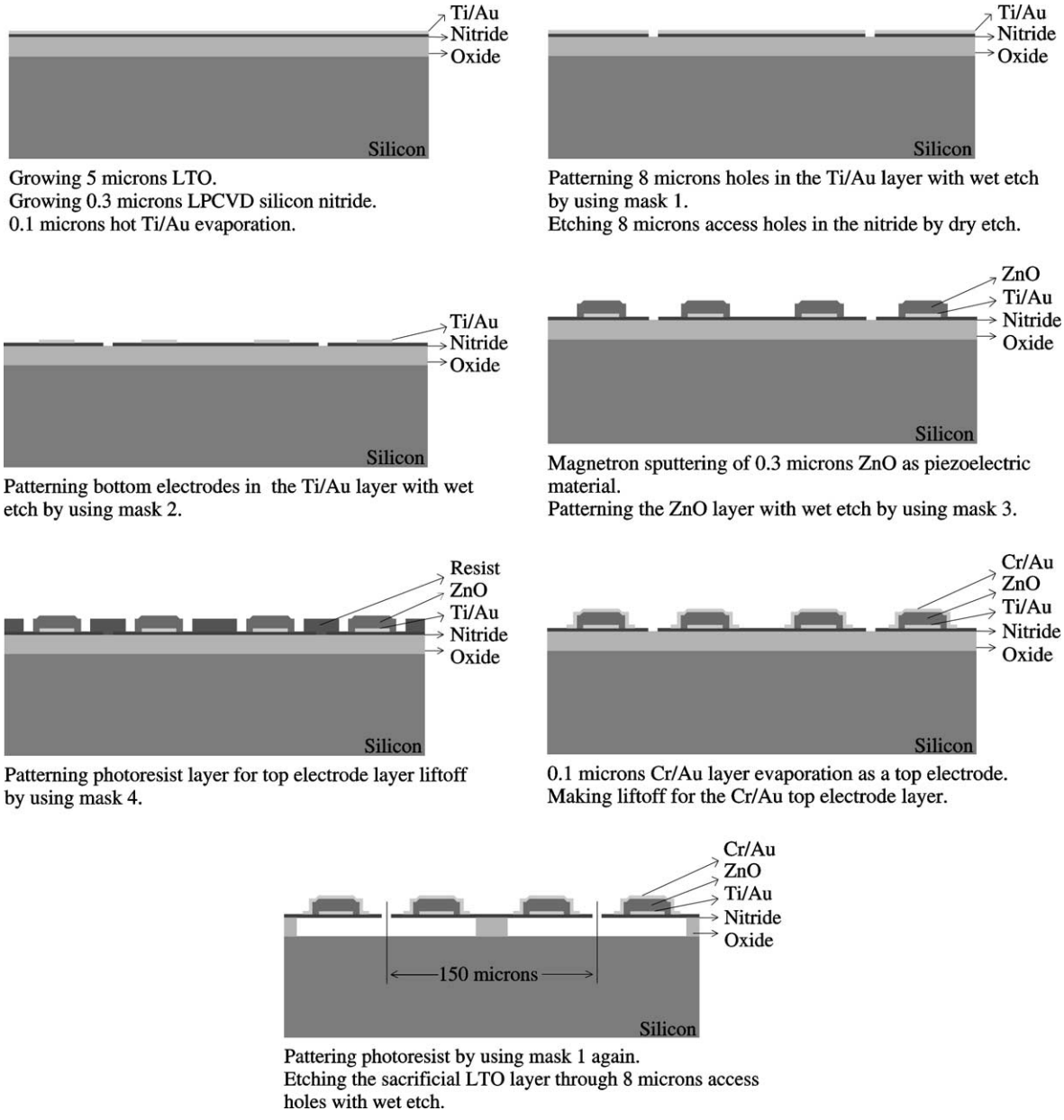

Fig. 6. First micromachined device process flow.

before defining the actual transducers at the front surface of the wafer. The bottom Ti/Au electrode layer is deposited on the non-piezoelectric carrier plate by e-beam evaporation at relatively high temperature. Later, the bottom electrode layer is patterned by wet etch, and a piezoelectric ZnO layer is deposited on top of the bottom electrode. The top Cr/Au electrode layer is formed by e-beam evaporation at room temperature and patterned by liftoff. The last step is etching the sacrificial layer by wet etch, and this concludes the front surface micromachining of the developed devices.

In the developed micromachining processes, ZnO is used as a piezoelectric material; however, other piezoelectric thin film materials can replace ZnO. These piezoelectric thin film materials can be relaxor-based piezoelectric single crystals, sol–gel PZT, sputtered PZT, and etc.

4. Experiments

Fig. 8 shows realized micromachined device and individual cells are 100 μm in diameter. By using the fabricated device, shown in Fig. 7, which has 4 cells connected in parallel, 100 μm-diameter thru-wafer backside access holes were filled with water, and a conventional

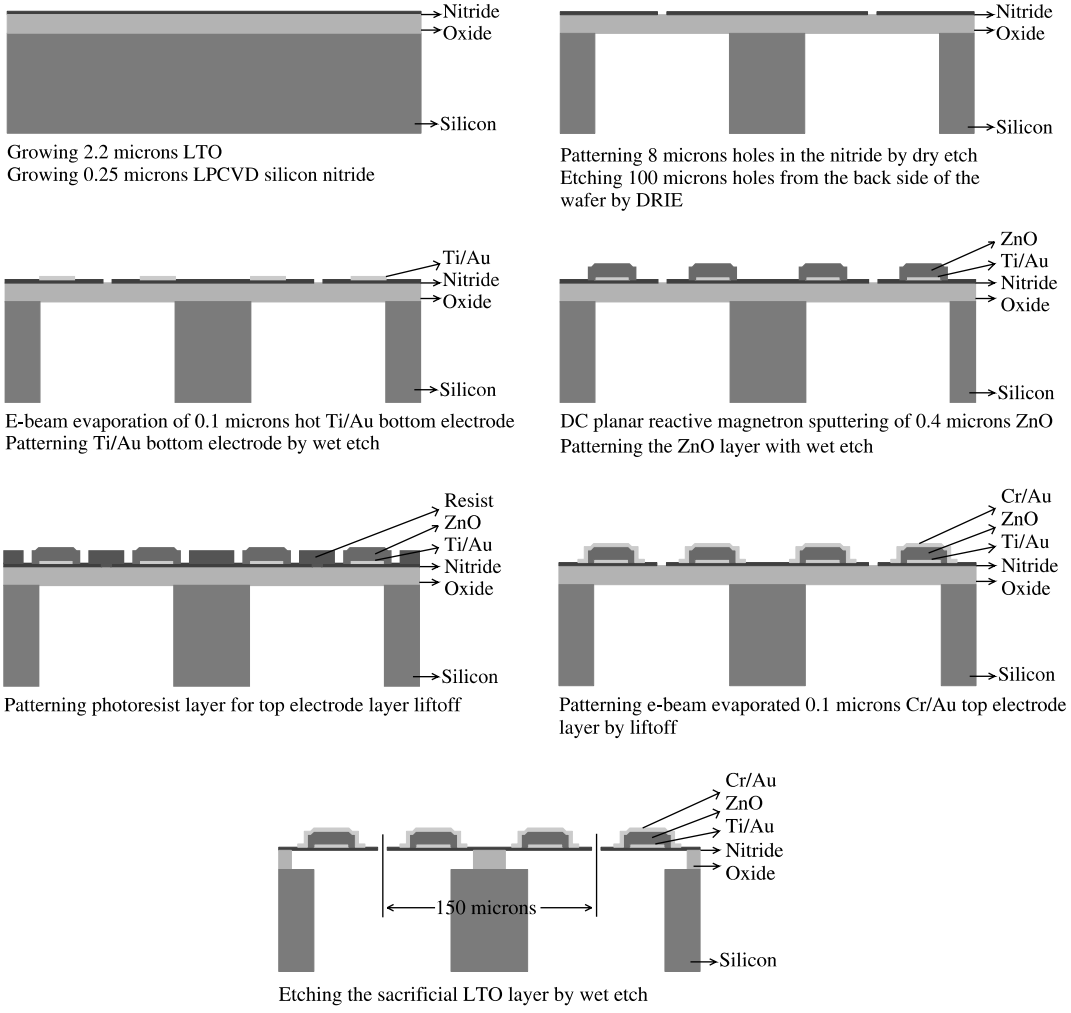

Fig. 7. The second micromachined device process flow.

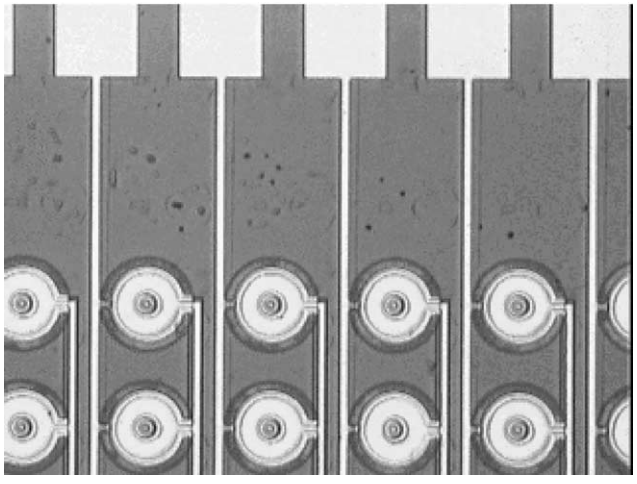

Fig. 8. Realized micromachined device: individual cells are 100 μm in diameter.

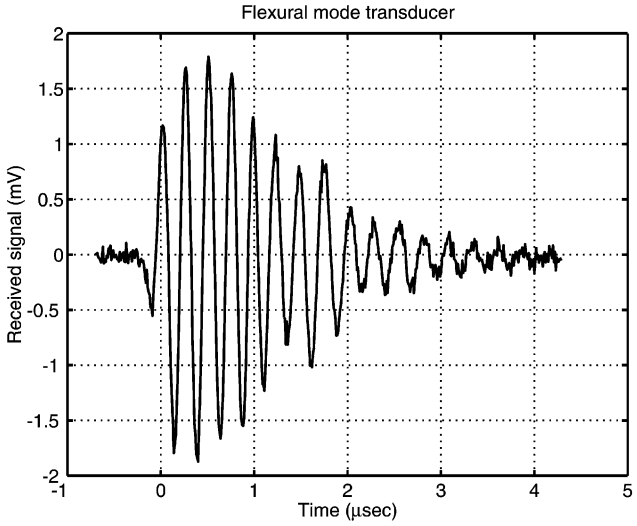

Fig. 9. Received signal at the flextensional transducer element.

longitudinal thickness mode transducer was used to excite ultrasound waves in air at 4 MHz. The longitudinal mode transducer was driven with a sinusoidal tone burst with four cycles at 4 MHz. In Figs. 9 and 10,

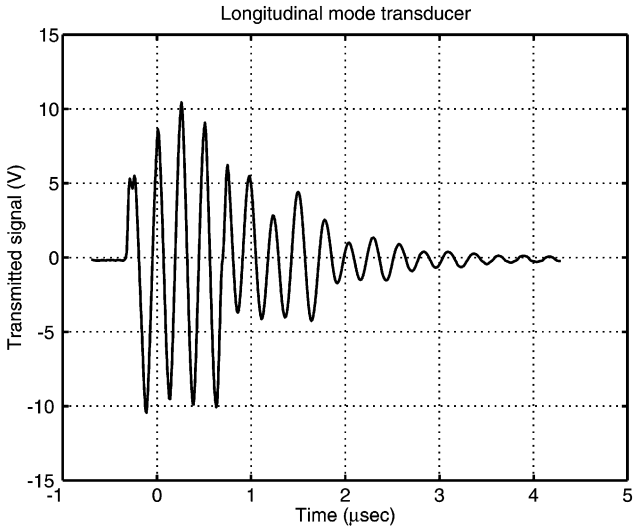

Fig. 10. Transmitted signal at the longitudinal mode transducer.

the received signal at the transducer and the transmitted signal at the longitudinal mode transducer are shown. As seen in Fig. 9, the device has a fractional bandwidth of 10% when loaded with water. Fig. 9 demonstrates the acoustical or, equivalently, electromechanical activity in the devices when they are loaded with fluid. In the experiments, a low noise amplifier with a gain of 25 (28 dB) was used to amplify the received signal at the device. Figs. 11–13 presents the real parts of the electrical input impedance measurements of the device for air, water and isopropanol (IPA) loaded cases. As shown in Figs. 11–13, the resonances shift down in frequency and become relatively broadband (25%) when the device is loaded with a fluid. The shift in resonance for the water loaded transducer is more than the one for

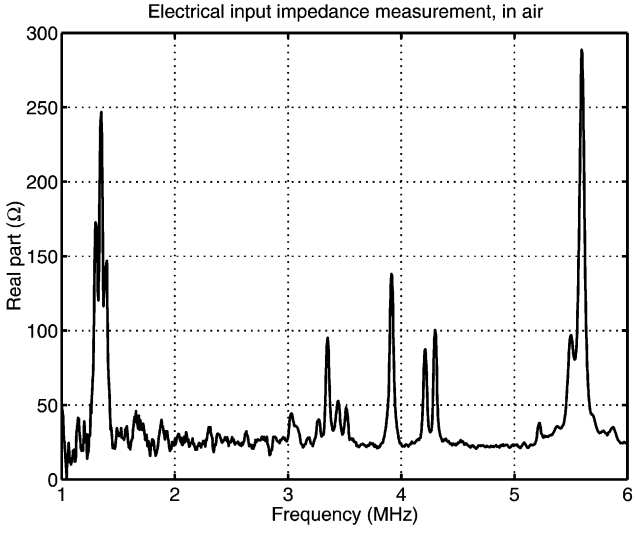

Fig. 11. Electrical input impedance of the flextensional transducer element (4 cells connected in parallel) when operating in air.

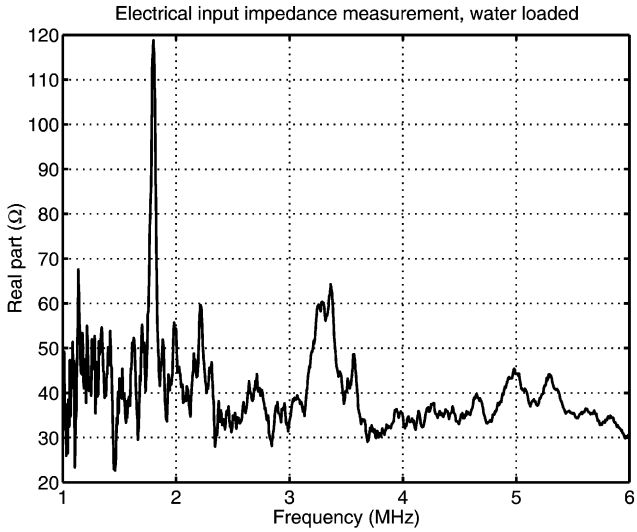

Fig. 12. Electrical input impedance of the flextensional transducer element (4 cells connected in parallel) when loaded with water.

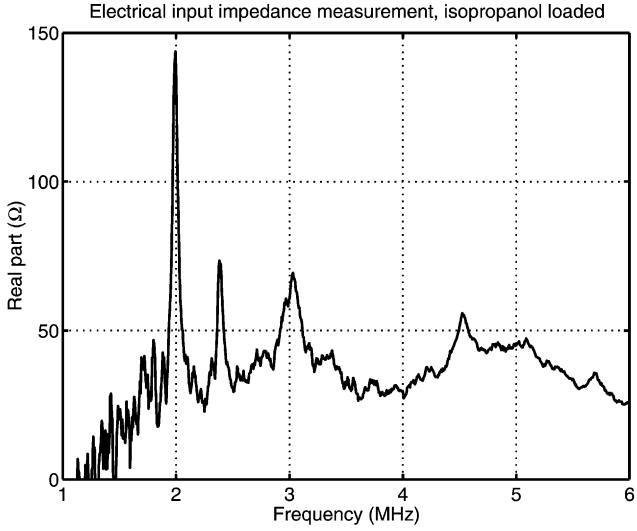

Fig. 13. Electrical input impedance of the flextensional transducer element (4 cells connected in parallel) when loaded with IPA.

IPA loaded case due to the fact that acoustic impedance of water is larger than the one for IPA. Another important point in Figs. 12 and 13 is the fact that the quality factor for the second resonance for fluid loaded cases is still relatively high, and this is because of the fact that the third mode has relatively small coupling to the surrounding medium. This can be easily seen from the simulated electrical input impedance, average displacement and mode shapes shown in Figs. 3, 4 and 14. As a result, one can say that some resonant modes are suitable for ultrasound transducer applications, such as imaging, nondestructive evaluation, etc., and some resonant modes are suitable for fluid ejection applications due to reduced acoustic coupling to the surrounding medium,

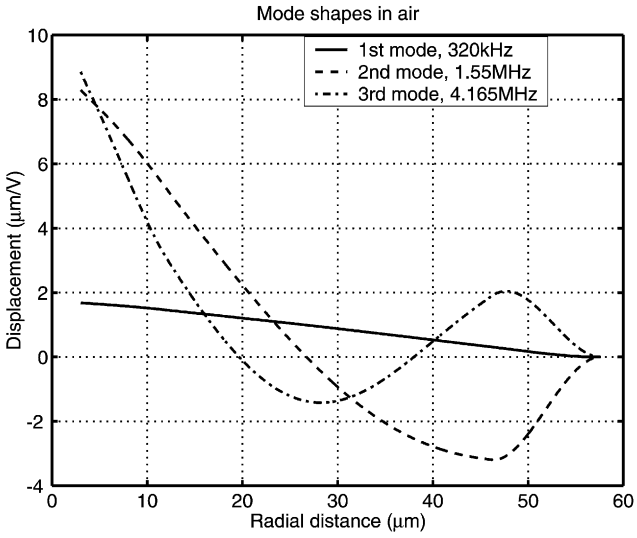

Fig. 14. Mode shapes of the single flextensional transducer cell.

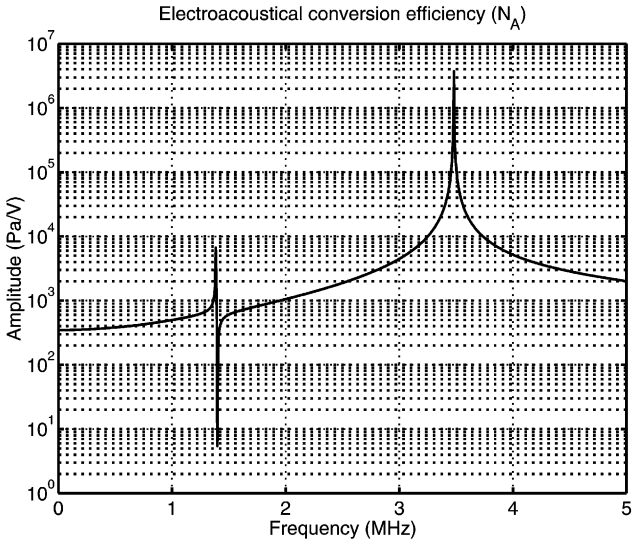

Fig. 16. Electroacoustical conversion efficiency (N_A) of the single flextensional transducer cell.

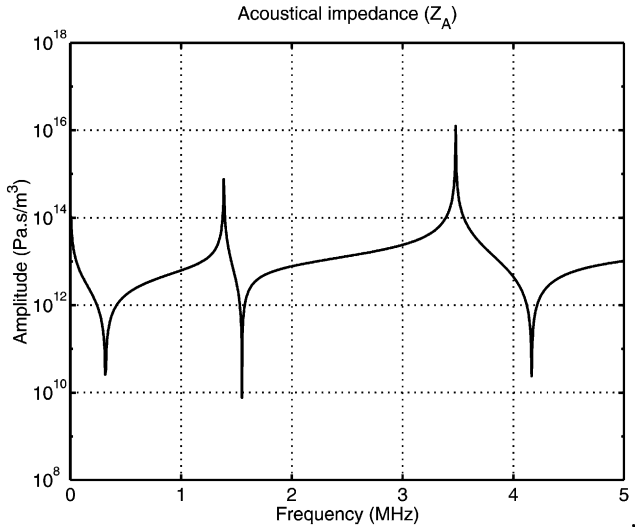

Fig. 15. Acoustical impedance (Z_A) of the single flextensional transducer cell.

but still large displacement. Finally, the acoustical impedance (Z_A) and electroacoustical conversion efficiency (N_A) of the device are given in Figs. 15 and 16.

5. Conclusion

In summary, we have developed a novel ultrasonic transducer, which is silicon micromachined into two-dimensional arrays. The individual cell design is based on a variation of a flextensional transducer. The transducer design was optimized initially using finite element analysis, but later using the model developed by Perçin and Khuri-Yakub [13] and the ultrasonic transmission was demonstrated in air and water.

References

[1] G. Perçin, L. Levin, B.T. Khuri-Yakub, Piezoelectrically actuated droplet ejector, Review of Scientific Instruments 68 (12) (1997) 4561–4563.

[2] G. Perçin, A. Atalar, F.L. Degertekin, B.T. Khuri-Yakub, Micromachined two dimensional array piezoelectrically actuated transducers, Applied Physics Letters 72 (11) (1998) 1397–1399.

[3] G. Perçin, T.S. Lundgren, B.T. Khuri-Yakub, Controlled ink-jet printing and deposition of organic polymers and solid-particles, Applied Physics Letters 73 (16) (1998) 2375–2377.

[4] B.T. Khuri-Yakub, L. Levin, Fluid drop ejector and method, US Patent Serial No. 5,828,394, issued October 27, 1998.

[5] G. Perçin, B.T. Khuri-Yakub, Micromachined two-dimensional array of piezoelectrically actuated flextensional transducers, US Patent Serial No. 6,291,927, issued September 18, 2001.

[6] G. Perçin, B.T. Khuri-Yakub, Micromachined two-dimensional array droplet ejectors, US Patent Application Serial No. 09/791,991, filed February 22, 2001.

[7] C.P. Germano, Flexure mode piezoelectric transducers, IEEE Transactions on Audio and Electroacoustics AU-19 (1973) 6–12.

[8] W.J. Denkmann, R.E. Nickell, D.C. Stickler, Analysis of structural-acoustic interactions in metal-ceramic transducers, IEEE Transactions on Audio and Electroacoustics AU-21 (4) (1973) 317–324.

[9] A.M. Allaverdiev, N.B. Akhmedov, T.D. Shermergor, Coupled flexural-shear oscillations of stepwise-layered piezoceramic disk transducers, Prikladnaya Mekhanika 23 (5) (1987) 59–66 (Russian).

[10] M.E. Vassergiser, A.N. Vinnichenko, A.G. Dorosh, Calculation and investigation of flexural-mode piezoelectric disk transducers on a passive substrate in reception and radiation, Soviet Physics Acoustics 38 (6) (1992) 558–561.

[11] H. Okada, M. Kurosawa, S. Ueha, M. Masuda, New airborne ultrasonic transducer with high output sound pressure level, Japan Journal of Applied Physics, Part I 33 (5B) (1994) 3040–3044.

[12] A. Iula, N. Lamberti, G. Caliano, M. Pappalardo, A matrix model of the thin piezoceramic ring, in: Proceedings of 1994 IEEE Ultrasonics Symposium, 1994, pp. 921–924.

[13] G. Perçin, B.T. Khuri-Yakub, Piezoelectrically actuated flextensional micromachined ultrasound transducers I: Theory, IEEE Transactions on Ultrasonics, Ferroelectrics, and Frequency Control 49 (4) (2002), in press.
[14] G. Perçin, B.T. Khuri-Yakub, Piezoelectrically actuated flextensional micromachined ultrasound transducers II: Fabrication and experiments, IEEE Transactions on Ultrasonics, Ferroelectrics, and Frequency Control 49 (4) (2002), in press.
[15] G. Perçin, B.T. Khuri-Yakub, Piezoelectrically actuated flextensional micromachined ultrasound droplet ejectors, IEEE Transactions on Ultrasonics, Ferroelectrics, and Frequency Control 49 (4) (2002), in press.